

FDTD Simulated Observation of a Gold Nanorod by Scanning Near-Field Optical Microscopy

Keiji SAWADA, Hiroaki NAKAMURA¹⁾, Teruto MARUOKA, Yuichi TAMURA²⁾, Kohei IMURA³⁾, Toshiharu SAIKI⁴⁾ and Hiromi OKAMOTO⁵⁾

Shinshu University, 4-17-1 Wakasato, Nagano 380-8553, Japan

¹⁾*National Institute for Fusion Science, 322-6 Oroshi-cho, Toki 509-5292, Japan*

²⁾*Konan University, 8-9-1 Okamoto, Higashinada-ku, Kobe 658-8501, Japan*

³⁾*Waseda University, 3-4-1 Okubo, Shinjyuku, Tokyo 169-8555, Japan*

⁴⁾*Keio University, 3-14-1 Hiyoshi, Kohoku-ku, Yokohama 223-8522, Japan*

⁵⁾*Institute for Molecular Science, 38 Myodaiji, Okazaki 444-8585, Japan*

(Received 7 December 2009 / Accepted 25 February 2010)

The optical properties of a gold nanorod were investigated by Imura *et al.* [J. Chem. Phys. **122**, 154701 (2005)] using an apertured-type scanning near-field optical microscope (SNOM). The observed transmission image showed an oscillating pattern along the long axis of the nanorod. We obtain the image using the finite-difference time-domain (FDTD) method. Our model includes a nanorod on a glass substrate, a SNOM, and current as a light source. We develop a simple method for including the Drude-Lorentz dispersion relation of Vial *et al.* [Phys. Rev. B **71**, 085416 (2005)] for gold in the FDTD. The oscillating pattern is explained by the total current in the nanorod, tip of the SNOM, and light source.

© 2010 The Japan Society of Plasma Science and Nuclear Fusion Research

Keywords: FDTD, SNOM, gold nanorod, plasmon, Drude-Lorentz model

DOI: 10.1585/pfr.5.S2110

1. Introduction

The study of optical phenomena related to the electromagnetic response of metals is growing rapidly and is concerned mostly with controlling optical radiation on the sub-wavelength scale. Gold nanorods have received considerable attention from the standpoint of electric field enhancement [1]. Imura *et al.* investigated the optical properties of gold nanorods using an aperture-type scanning near-field optical microscope (SNOM) [2–4]. The observed transmission images show an oscillating pattern along the long axis of the nanorod. These spatial characteristics were explained by local density of states (LDOS) maps, leading to a fundamental understanding of the images. However, the details of the electromagnetic interaction between the nanorod and the surface of the SNOM tip were not considered in the discussion. A study of the interaction between the nanorod and the SNOM is still needed.

In this paper, we construct a code based on the finite-difference time-domain (FDTD) method [5–7]. We develop a simple method to include the Drude-Lorentz dispersion relation of gold [8] in the FDTD. We investigate the origin of the oscillating pattern found experimentally.

2. Model

The Au-coated double-tapered probe used in the experiment [2–4] is reproduced in our FDTD model, as il-

lustrated in Fig. 1. Computational domains of $6.7 \times 6.7 \times 11.119 \mu\text{m}^3$ are divided into $350 \times 350 \times 451$ cells. The lattice space increments are 2–50 nm. The tip of the probe and the nanorod are divided into 2-nm cells. We use the Mür absorbing boundary [5] for the top and bottom boundaries in Fig. 1 and a periodic boundary for the side boundaries to suppress noise from the boundaries. We determine the size of the computational domain to secure a time region in which noise from the boundaries does not affect the cal-

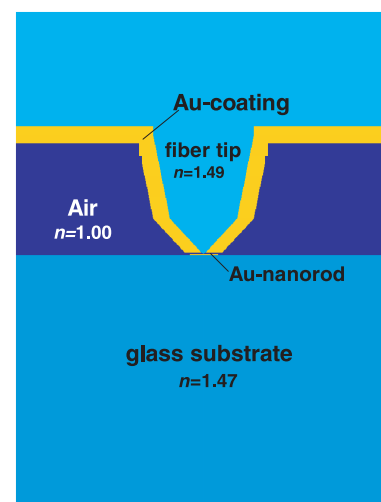


Fig. 1 Computational domain. n indicates the refractive index.

author's e-mail: ksawada@shinshu-u.ac.jp

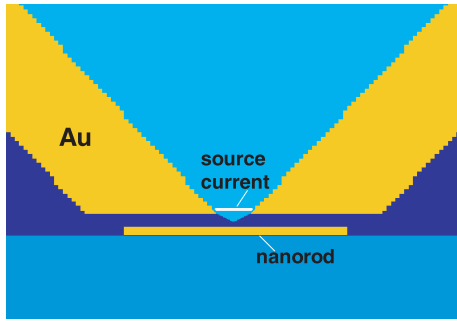


Fig. 2 Tip of the probe and the nanorod.

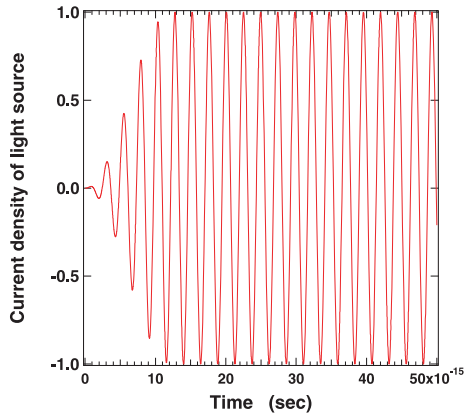


Fig. 3 Current density of the light source.

culation of the nanorod image, as explained below. The length and diameter of the nanorod are 510 nm and 20 nm, respectively. The aperture diameter of the probe tip used in the experiment is estimated to be in the range of 50–100 nm [2–4]. In the present model, it is set to 80 nm. The z -axis is defined as the axis of the probe and the x -axis as the long axis of the nanorod.

The wavelength of incident light is 730 nm. The source current is placed within a radius of 40 nm at the tip of the probe (Fig. 2) to produce the light. The source current oscillates parallel to the long axis of the nanorod. As shown in Fig. 3, the intensity of the current density of the source gradually increases and is saturated within five periods to eliminate the high-frequency component.

The dispersion of gold in the nanorod and the surface of the probe tip is modeled according to the Drude-Lorentz model in Ref. [8], which is accurate in the wavelength range 500–1000 nm.

For gold, the Maxwell equations solved in the FDTD are

$$\begin{aligned}
 \frac{\partial \mathbf{E}}{\partial t} &= \frac{1}{\epsilon_0} \text{rot } \mathbf{H} - \frac{1}{\epsilon_0} \mathbf{J} \\
 &= \frac{1}{\epsilon_0} \text{rot } \mathbf{H} - \frac{1}{\epsilon_0} \frac{\partial \mathbf{P}}{\partial t}, \quad (1)
 \end{aligned}$$

$$\frac{\partial \mathbf{H}}{\partial t} = -\frac{1}{\mu_0} \text{rot } \mathbf{E}. \quad (2)$$

The Drude-Lorentz model is used to calculate the cur-

Table 1 Values of the parameters used in Eq. (3).

Parameters	Values
ϵ_∞	$5.9673\epsilon_0$
$\omega_D/2\pi$ (THz)	2113.6
$\gamma_D/2\pi$ (THz)	15.92
$\Omega_L/2\pi$ (THz)	650.07
$\Gamma_L/2\pi$ (THz)	104.86
$\Delta\epsilon$	1.09

rent density \mathbf{J} or dipole moment \mathbf{P} in gold. The absolute permittivity of gold is given as

$$\epsilon_{DL}(\omega) = \epsilon_\infty - \frac{\epsilon_0 \omega_D^2}{\omega(\omega + i\gamma_D)} - \frac{\epsilon_0 \Delta\epsilon \Omega_L^2}{(\omega^2 - \Omega_L^2) + i\Gamma_L \omega}, \quad (3)$$

where the values of the parameters are listed in Table 1. The first, second, and third terms on the right-hand side of Eq. (3) originate from the instantaneous permittivity, Drude model, and Lorentz model, respectively.

We transform Eq. (3) into the following differential equations. The differential equation for the Lorentz model is written as

$$\frac{\partial^2 \mathbf{P}_L}{\partial t^2} + \Gamma_L \frac{\partial \mathbf{P}_L}{\partial t} + \Omega_L^2 \mathbf{P}_L = \epsilon_0 \Delta\epsilon \Omega_L^2 \mathbf{E}. \quad (4)$$

In the present FDTD model, this equation is solved as a set of coupled differential equations,

$$\frac{\partial \mathbf{J}_L}{\partial t} + \Gamma_L \mathbf{J}_L = \epsilon_0 \Delta\epsilon \Omega_L^2 \mathbf{E} - \Omega_L^2 \mathbf{P}_L, \quad (5)$$

$$\frac{\partial \mathbf{P}_L}{\partial t} = \mathbf{J}_L. \quad (6)$$

The differential equation for the Drude model is written as

$$\frac{\partial \mathbf{J}_D}{\partial t} + \gamma_D \mathbf{J}_D = \epsilon_0 \omega_D^2 \mathbf{E}. \quad (7)$$

The dipole moment in Eq. (1) is given as

$$\mathbf{P} = (\epsilon_\infty - \epsilon_0) \mathbf{E} + (\mathbf{P}_D + \mathbf{P}_L). \quad (8)$$

Using Eqs. (5), (6), (7), and (8), we rewrite Eq. (1) as

$$\frac{\partial \mathbf{E}}{\partial t} = \frac{1}{\epsilon_\infty} \text{rot } \mathbf{H} - \frac{1}{\epsilon_\infty} (\mathbf{J}_D + \mathbf{J}_L). \quad (9)$$

We solve Eqs. (2), (5), (6), (7), and (9) to calculate the electromagnetic fields and current density in gold.

3. Results and Discussion

Figure 4 shows the experimental transmission image of the nanorod obtained by SNOM [2–4]. The wavelength of the incident light was 729 nm. The transmission was defined as

$$\Delta T = \frac{I_0 - I}{I_0}, \quad (10)$$

where I and I_0 represent the observed light intensities with and without the nanorod, respectively. The lens and detector were located under a 0.15-mm-thick glass substrate.

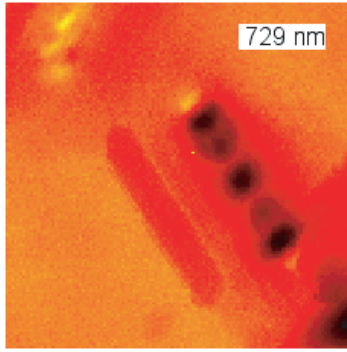


Fig. 4 Transmission image of gold nanorod observed by SNOM [2–4] (see Fig. 7 for transmission along the long axis of the nanorod).

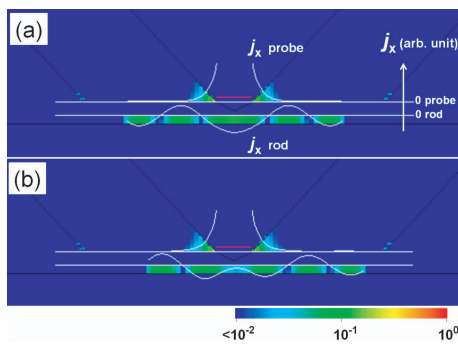


Fig. 5 Magnitude of the x component of current density j_x in gold in the x - z plane at 44.44×10^{-15} s. Nanorod shift: (a) 0 nm, (b) 50 nm. White curves show the relative value and direction of the current density in the top surface of the nanorod and in the flat tip surface of the probe. Zero lines are drawn at both surfaces. Positive values are plotted in the upward direction.

Linearly polarized light in the x direction was detected with a polarizing filter.

In the calculation, the nanorod is placed at a position where its center is on the axis of the probe and shifted along the direction of the long axis of the nanorod in 50-nm steps. The FDTD calculation is performed for each position of the nanorod.

Examples of the calculated current density in gold are given in Figs. 5 (a) and (b). The x component of the current density in the x - z plane at the source current peak of 44.44×10^{-15} s is shown for rod shifts of 0 nm and 50 nm. Plasmons in the nanorod are clearly seen. Figures 6 (a) and (b) show the x component of the current density in the y - z plane at the same time. The direction of the current density in the probe's surface is opposite to that of the current source.

Because the detector cannot be included in the computational domain, we calculate the intensity I from the current density in the nanorod, probe, and light source as follows: We calculate the total current in the nanorod, probe, and light source, and calculate the squared values of the

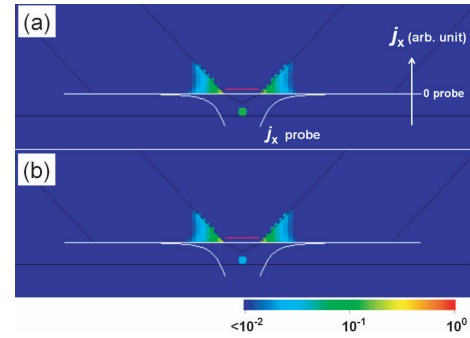


Fig. 6 Magnitude of the x component of current density j_x in gold in the y - z plane at 44.44×10^{-15} s. Nanorod shift: (a) 0 nm, (b) 50 nm. Color and j_x scales are the same as in Fig. 5.

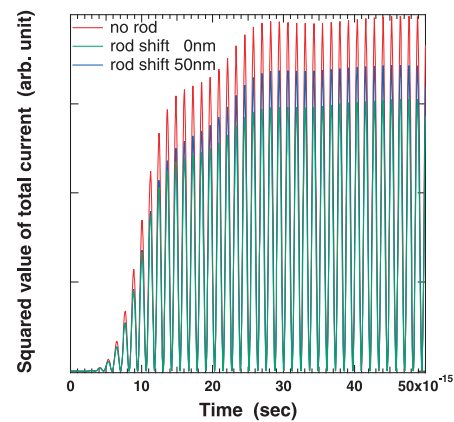


Fig. 7 Squared values of the total current for 0 nm and 50 nm rod shifts. Value with no nanorod is also shown.

total current as a function of time,

$$S(t) = \left(\sum_{R \leq 0.8 \mu\text{m}} j_x(t) \Delta V \right)^2, \quad (11)$$

where $j_x(t)$ is the x component of the current density vector. ΔV is the volume of each FDTD cell. The current densities within a radius of $0.8 \mu\text{m}$ are summed. The current densities outside the radius are negligible, and the resolution of the experimental optical system [2–4] is estimated to be larger than the radius. Figure 7 shows $S(t)$ for rod shifts of 0 nm and 50 nm. The total current for a 0-nm rod shift is smaller than that for a 50-nm rod shift. The result here is consistent with the image in the central region of Fig. 4.

We calculate the average of the peak values in the steady time region of 40–50 fs in Fig. 7. This value is expected to be proportional to the experimentally observed light intensity I to a good approximation. Figures 8 (a) and (b) show the calculated x component of the current density in gold at the peak time of 44.03×10^{-15} s in Fig. 7 for rod shifts of 0 nm and 50 nm, respectively.

Figure 9 shows the calculated and experimental trans-

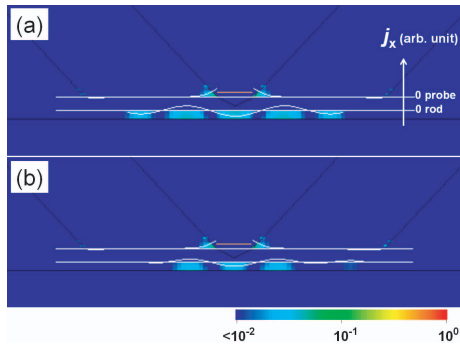


Fig. 8 Magnitude of the x component of current density j_x in gold in the x - z plane at 44.03×10^{-15} s. Nanorod shift: (a) 0 nm, (b) 50 nm. Color and j_x scales are the same as in Fig. 5.

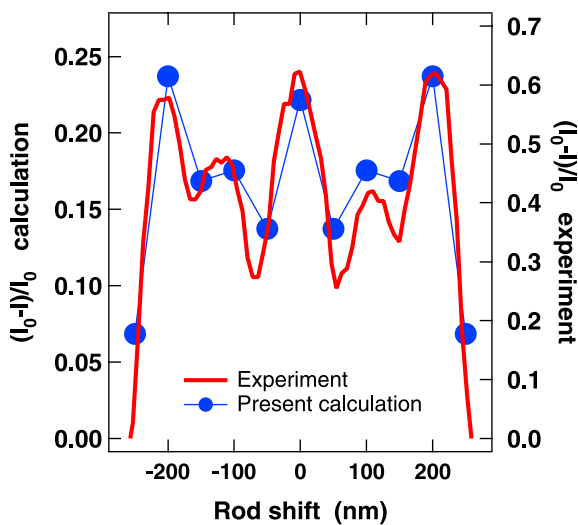


Fig. 9 Transmission along the long axis of the nanorod. Calculated and experimental values [2–4] are shown.

mission values along the long axis of the nanorod. The calculation reproduces the experimental oscillating pattern well. The disagreement in the calculated and experimental

absolute values may be attributed to the difference in the effective diameter of the near-field light source.

4. Conclusion

The experimentally observed oscillating pattern in transmission images along the long axis of a gold nanorod was reproduced by the Drude-Lorentz FDTD method, which includes a nanorod on a glass substrate, a SNOM, and a light source. In the present study, we developed simple methods to include the dispersion of gold and calculate the far-field signal. The experimental oscillating pattern arises from the total current in the nanorod, probe, and light source. The effectiveness of the present modeling for calculating the image of the nanorod by SNOM is confirmed.

Acknowledgment

The authors thank I. Fukushima, K. Ikushima, and M. Shibata for their assistance in constructing the code. This work was supported by the National Institutes of Natural Sciences undertaking Forming Bases for Interdisciplinary and International Research through Cooperation Across Fields of Study and Collaborative Research Program (No. NIFS09KEIN0121).

- [1] C. Sönnichsen, T. Franzl, T. Wilk, G. von Plessen, J. Feldmann, O. Wilson and P. Mulvaney, *Phys. Rev. Lett.* **88**, 077402-1-4 (2002).
- [2] K. Imura, T. Nagahara and H. Okamoto, *J. Chem. Phys.* **122**, 154701 (2005).
- [3] K. Imura and H. Okamoto, *Opt. Lett.* **31**, 1474 (2006).
- [4] H. Okamoto and K. Imura, *J. Mater. Chem.* **16**, 3920 (2006).
- [5] K. Kunz and R. Luebbers, *The Finite Difference Time Domain Method for Electromagnetics*. (CRC Press, 1993).
- [6] K. Sawada, M. Sakai, Y. Kohashi, T. Saiki and H. Nakamura, *J. Plasma Phys.* **72**, 1019 (2006).
- [7] K. Sawada, H. Nakamura, H. Kambe and T. Saiki, *IEICE Tran. Electron.* **E85-C**, 2055 (2002).
- [8] Alexandre Vial, Anne-Sophie Grimault, Demetrio Macias, Dominique Barchiesi, and Marc Lamy de la Chapelle, *Phys. Rev. B* **71**, 085416 (2005).